J Mater Sci (2007) 42:179–184
DOI 10.1007/s10853-006-0845-6

Effect of matrix structure on ultrasonic attenuation of ductile cast iron

Xinbao Liu · Susumu Takamori · Yoshiaki Osawa

Received: 2 March 2005 / Accepted: 1 November 2005 / Published online: 5 December 2006

Abstract The ultrasonic attenuation of ductile cast irons with different matrices was investigated by means of ultrasonic echo waves. In the ductile cast irons with ferritic and pearlitic matrix structures, both of the ultrasonic attenuation increased with frequency. For similar frequencies, the ultrasonic attenuation of the pearlitic matrix was larger than that of the ferritic matrix. Based on the theory of ultrasonic attenuation in the solid, the mechanisms of ultrasonic attenuation in the ductile cast irons with different matrices were analyzed. It indicated that in the ductile cast irons with transformation of matrix from the ferrite to the pearlite, the mechanism of ultrasonic attenuation varied in the range of present frequencies. In the ferritic matrix, the total ultrasonic attenuation was mainly attributed to the scattering loss which included the stochastic scattering and the Rayleigh scattering. On the contrary, the absorption loss predominated in the total ultrasonic attenuation of the ductile cast iron with pearlitic matrix.

Introduction

Ductile cast iron is a useful engineering material due to its excellent mechanical properties, such as strength, ductility and plasticity [1]. Besides, different matrix structures can be easily obtained by heat treatment processing. The ferritic matrix is more machinable and ductile, while the pearlitic matrix exhibits better strength and more wear-resistant. Due to different properties of the two types of ductile cast irons, it is necessary to determine the matrix structure during the process of producing ductile cast iron as soon as possible. As propagation of the ultrasonic wave depends largely upon the microstructure of materials, ultrasonic attenuation can be a desired parameter for characterization of ductile cast irons with different matrix structures.

The previous experiments indicated that the ultrasonic attenuation is correlated with microstructures in steels [2] and other materials [3, 4]. Besides, Lee et al. [5] have used the ultrasonic technique for determination of the relationship of nodularity and matrix with ultrasonic characteristics of cast irons. Their experiment results showed that the ultrasonic velocity and attenuation is very useful for determination of the nodularity and the microstructure. In their experiments, however, the measurements of ultrasonic attenuation were only a qualitative description, which can't clarify the influence of matrix structure on ultrasonic attenuation of cast irons in detail.

In the present work, we applied the ultrasonic technique to measure the ultrasonic attenuation of ductile cast irons with different matrix structures. Combined with the theory of ultrasonic attenuation in the solid, the effect of matrix structure on the ultrasonic attenuation of ductile cast irons was discussed. It was expected that the present measurement of ultrasonic attenuation could be an important metallurgical and quality-control tool in the foundries producing high-quality castings.

X. Liu (✉) · S. Takamori · Y. Osawa
Eco-Circulation Processing Materials Group, National Institute for Materials Science, Tsukuba, Ibaraki 305-0047, Japan
e-mail: liu.xinbao@nims.go.jp

Experimental methods

The ingot of ductile cast iron made with continuous casting was provided by Satake Special Steel Corp., Japan. The chemical composition of it is listed in Table 1. In order to obtain the ductile cast irons with ferritic and pearlitic matrices, different heat treatments were carried out. To avoid oxidation and decarburization, all specimens were placed in a sealed stainless-steel can, which was filled with graphite powders and iron shavings. During the processing of heat treatments, specimens were initially held at 900 K for an hour and then cooled to room temperature with different rates to obtain the ferritic and pearlitic matrices.

Measurements of ultrasonic attenuation were carried out by an apparatus made by Toshiba Tungaloy, Japan. Figure 1 illustrates the schematic of the system of ultrasonic measurement. A pulse-receiver with 100 MHz broad band was used to transmit the electrical pulse to the transducer for generating ultrasonic waves. A longitudinal-broadband transducer (Toshiba Tungaloy, Japan) with a central frequency of 5 MHz was used to generate ultrasonic waves. In order to avoid the non-uniform amplitude in the near field of transducer, a buffer rod (fused silica) was employed to provide time delay between the excitation pulse and echoes returning from the measured sample.

The schematic of propagation of the longitudinal wave are shown in Fig. 2. The specimen is of length L,

Table 1 Chemical composition of the ingot (wt. %)

C	Si	Mn	P	S	Mg	Fe
3.48	3.15	0.24	0.023	0.007	0.037	Bal.

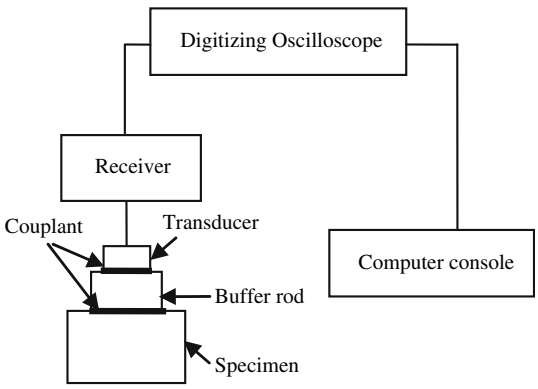

Fig. 1 Schematic of the experimental setup for ultrasonic measurements

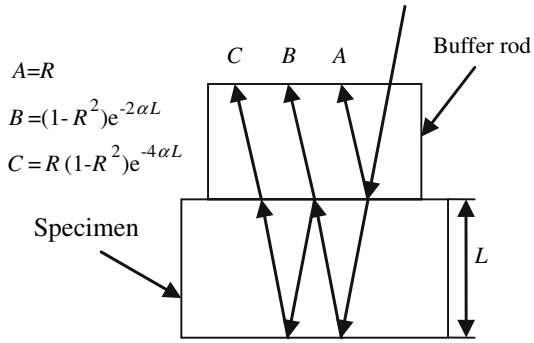

Fig. 2 Diagram of reflections from and within a sample attached to buffer rod. The relative amplitudes A, B and C are given in terms of the refection coefficient R, the attenuation α, and the sample thickness, L

longer than the ultrasonic wave length to be employed. A wave generated by the transducer follows the paths of partial reflection and transmission, giving rise to echoes A, B and C in the buffer rod. Let A, B and C denote amplitudes of the three separate echoes in a sample, respectively. According to the Ref.6, let A and C be normalized by division by B, such that

$$\tilde{A} = A/B \tag{1}$$

and

$$\tilde{C} = C/B \tag{2}$$

Based on Eqs. of (1) and (2), it can be obtained that the reflection coefficient, R, of the surface between the buffer rod and the measured specimen has the following expression

$$R = \sqrt{\frac{\tilde{A}\tilde{C}}{1+\tilde{A}\tilde{C}}} \tag{3}$$

Combined with the definition of ultrasonic attenuation coefficient, it can be obtained that

$$\alpha = \frac{20\log(R/\tilde{C})}{2L} \tag{4}$$

where L is the sample thickness. In general, the frequency-dependent attenuation coefficient $\alpha(f)$ is determined from the amplitude spectra of the three echo waveforms,

$$\alpha(f) = \frac{20\log(R(f)/\tilde{C}(f))}{2L} \tag{5}$$

where R(f) is the measured frequency-dependent reflection coefficient of the surface between the buffer

rod and specimen, which can be calculated by the amplitude spectra of the three echoes, $A(f)$, $B(f)$ and $C(f)$ with equations (1–3). $\tilde{C}(f)$ is the normalized frequency-dependent amplitude spectrum of $C(f)$. Besides, the valid frequency range is determined from the amplitude spectrum of $C(f)$ [6].

In practical measurements, the beam diffraction usually caused appreciable additions to the ultrasonic attenuation as measured by pulse-echo method [7, 8]. In order to avoid the effect of diffraction on the echo waveforms, it was necessary to make corrections to the amplitude spectra of three echo waveforms. First, a normalized distance, S, is calculated for each echo.

$$S = z\lambda/a^2 = zv/a^2 f \tag{6}$$

where z is the propagation distance, v the velocity, a the transducer radius and f the frequency. Then, from the curve [9] of dB vs. S, the amplitude spectra of three echo waveforms with diffraction correction, $A_0(f)$, $B_0(f)$ and $C_0(f)$, can be obtained. Consequently, the ultrasonic attenuation with diffraction correction can be achieved by Eqs. (1)–(3) and (5).

Before the measurement of ultrasonic attenuation, the surface grinding of samples was carried out to obtain the specimens of 15 ± 0.02 mm thickness with plane parallelism to an accuracy of better than ± 0.3 μm. Besides, the etched microstructures were examined by an optical microscope.

Results and discussion

Experiment results

Figure 3 gives the microstructure morphologies of ductile cast irons with different matrices. Fig. 3a is the microstructure of the ductile cast iron with ferritic matrix. In this micrograph, the average diameter of the dispersed spherical graphite is approximately 0.03 mm, which is much smaller than the ultrasonic wavelength, 1.09 mm, at a frequency of 5 MHz [5]. However, the grain size of inhomogeneous matrix far from the spherical graphite is close to above ultrasonic wavelength. The microstructure of the ductile cast iron with pearlitic matrix is shown in Fig.3b. Besides the dispersed spherical graphite, it is mainly composed of the gray pearlite with lamellar structures far from the spherical graphite and the remaining ferrite around the spherical graphite. The average diameter of spherical graphite is almost equal to that of the ductile cast iron with ferritic matrix. Compared with the ferrite in the ductile cast iron with ferritic matrix, the grain size of pearlitic matrix with lamellar structures is much smaller.

Figure 4 illustrates the relationship between ultrasonic attenuation and frequency in the ductile cast irons with different matrix structures. Obviously, it can be seen that both of ultrasonic attenuation in the ductile cast irons with ferritic and pearlitic matrices are sensitive to the frequency and increase with it in the

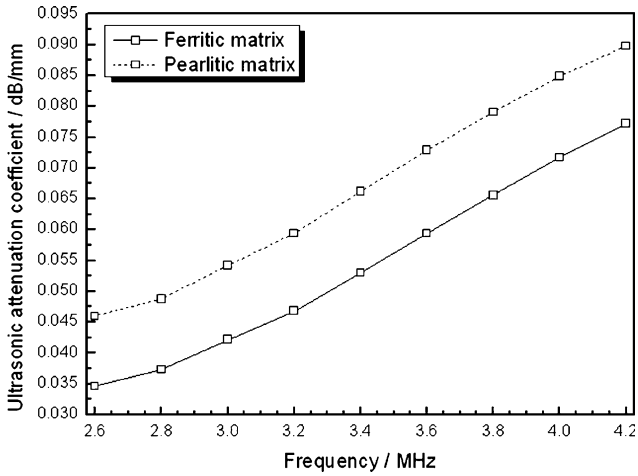

Fig. 4 Ultrasonic attenuation versus frequency in ductile cast irons with different matrix structures

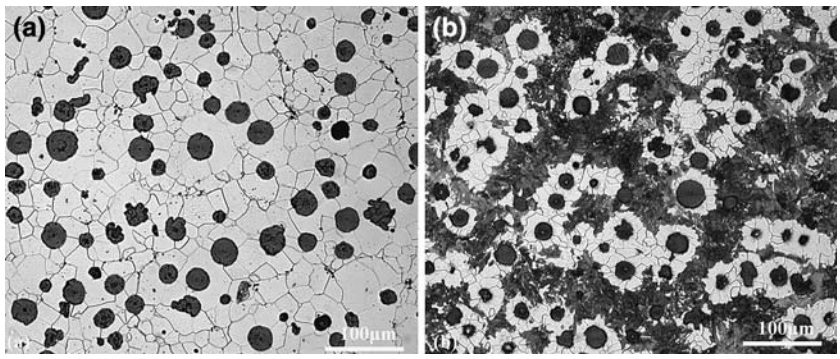

Fig. 3 Microstructures of ductile cast irons with different matrices, (**a**) ferritic matrix and (**b**) pearlitic matrix

range of present frequencies. The maximum ultrasonic attenuations, 0.077 dB/mm and 0.090 dB/mm, were obtained in the ductile cast irons with ferritic and pearlitic matrices, respectively. For similar frequencies, however, the ultrasonic attenuation in the ductile cast iron with pearlitic matrix is larger than that of the ferritic matrix.

By above experiment results, it can be seen that the ultrasonic attenuation varied in the ductile cast irons with the matrix structures from the ferrite to the pearlite. For similar frequencies, the ultrasonic attenuation of the ductile cast iron with pearlitic matrix is larger than that of the ferritic matrix. Besides, in the ductile cast irons with ferritic and pearlitic matrices, both of the ultrasonic attenuations increase with frequency in the range of present frequencies.

Discussion

The ultrasonic attenuation was mainly influenced by the microstructure of materials. By comparison of above microstructures of the ductile cast irons with ferritic and pearlitic matrices, it can be found that the appreciable difference is the formation of pearlite with lamellar structures. Therefore, it can be deduced that the increase in ultrasonic attenuation of the ductile cast iron with pearlitic matrix was related to these lamellar structures.

The attenuation during the propagation of ultrasonic wave in a solid material is composed of the absorption and the scattering loss [10]. The measured ultrasonic attenuation coefficient, α, is the sum of the absorption coefficient α_A and the scattering coefficient α_S, which can be written by

$$\alpha = \alpha_A + \alpha_S \tag{7}$$

The absorption process is attributed to the transformation of acoustic energy into thermal energy, which includes many interaction mechanisms, such as the internal friction caused by the dislocations and the thermoelasticity. Many experiments indicated that there is a linear relationship between the absorption coefficient and frequency [11, 12]. However, the scattering loss is particularly influenced by phase boundaries, which is caused by a jump in acoustic impendence ($\Delta\rho v$). It can be principally excited on the boundaries of phase, grain, inclusion and pore. Based on the previous theoretical derivations [13, 14], it indicated that when the average diameter of phase or the grain size, d, is much smaller than the ultrasonic wave length, λ, the scattering is in the Rayleigh scattering regions and can be evaluated by the expression

$$\alpha_S = Sd^3f^4 \tag{8}$$

where S is a constant, which is determined by the difference in acoustic impendence for phase boundaries or by the phase anisotropy for grain boundaries, respectively. When the average diameter of phase or the grain size is larger than the ultrasonic wave length, the scattering is in the stochastic scattering regions and can be calculated by

$$\alpha_S = \sum df^2 \tag{9}$$

where Σ is a constant, which is determined by the difference in acoustic impendence for phase boundaries. According to above analyses, Eq. 7 can be rewritten by the following form

$$\alpha = C_1 f + \sum df^2 + Sd^3f^4 = C_1 f + C_2 f^2 + C_3 f^4 \tag{10}$$

where C_1, C_2 and C_3 are constants for a fixed material. By Eq. 10, it is obvious that for similar frequencies, the values of constants C_1, C_2 and C_3 can represent the magnitudes of the absorption loss, the stochastic scattering loss and the Rayleigh scattering loss in different materials, respectively.

Combined with Eq. 7 and 10, the measured ultrasonic attenuation is composed of two components, the absorption loss and the scattering loss which included the stochastic scattering and the Rayleigh scattering loss. By calculation with the method of least squares, the values of C_1, C_2 and C_3 can be obtained for the ductile cast irons with different matrix structures, which are shown in Table 2. It can be seen that the constants of C_1 and C_3 in the ductile cast iron with pearlite matrix are much larger than those of the ferrite matrix, which indicated that the absorption loss and the Rayleigh scattering loss in the pearlite matrix are larger than those of ferrite matrix. However, the change of constant C_2 is contrary in the ductile cast irons with the matrix structures from the ferrite to the pearlite, which indicated that the stochastic scattering loss in the pearlite matrix is much smaller than that of

Table 2 Constants of C_1, C_2 and C_3 in ductile cat irons with different matrices

Matrix structure	C_1/Db/mm/MHz	C_2/dB/mm/MHz^2	$C_3/10^{-5}$ dB/mm/MHz^4
Ferrite	0.0045	0.0031	1.238
Pearlite	0.0130	0.0013	5.030

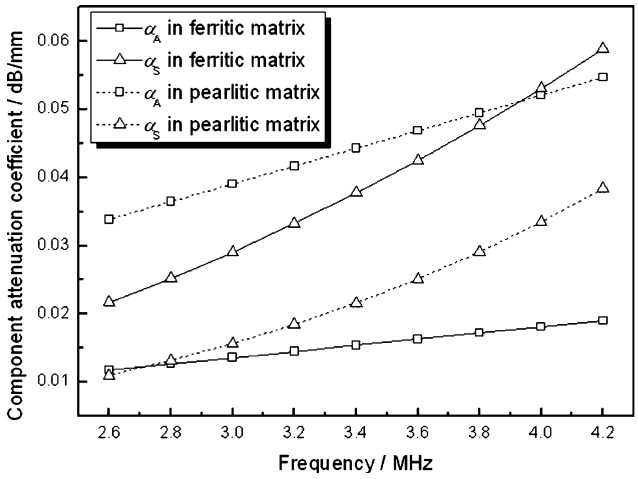

Fig. 5 Absorption loss and scattering loss versus frequency in ductile cast irons with different matrix structures

the ferrite matrix. Furthermore, Fig. 5 presents the two components of the absorption loss and the scattering loss with the increasing frequency in the ductile cast irons with different matrix structures. It is very clear that in both matrix structures of ductile cast irons, the two components of absorption loss and scattering loss increase with frequency. In the ductile cast iron with ferritic matrix, the ultrasonic attenuation is principally caused by the scattering loss. At the frequency of 4.2 MHz, the scattering loss is 76% of the total ultrasonic attenuation. On the contrary, in the ductile cast iron with pearlitic matrix, the ultrasonic attenuation is mainly attributed to the absorption loss which is 75% of the total ultrasonic attenuation at the frequency of 2.6 MHz. Besides, it can be known that compared with the ferritic matrix, the higher ultrasonic attenuation of the ductile cast iron with pearlitic matrix is mainly attributed to the large increase of absorption loss.

Generally, in the ductile cast iron systems, the absorption loss and the scattering loss are determined by many factors, respectively. The absorption loss is particularly related to the spherical graphite and dislocations existing in the matrix. Because there are no appreciable differences in the morphologies of spherical graphite for the both ductile cast irons, as shown in Fig. 3, the change of ultrasonic attenuation mechanism is predominately attributed to the formation of pearlite with lamellar structures. During the processing of pearlite heat treatment, the soft ferrite and the hard cementite alternately grew at high temperatures. Due to the volume dilation of transformation with rapid cooling velocity of temperature, it is very easy that many pinned dislocations existed within the ferrite boundaries near the interface of ferrite and cementite [15]. In the ductile cast iron with ferritic matrix, however, there were few dislocations due to the slow cooling velocity of temperature. Therefore, the absorption loss in the ductile cast iron with the pearlitic matrix was much larger than that of the ferrite matrix, which consequently brought increase of the total ultrasonic attenuation.

Furthermore, the other component of scattering loss is mainly influenced by the diameter of spherical graphite, the matrix grain size and the phase anisotropy in the ductile cast iron system. By above experiment results, it has been known that the difference in the diameter of spherical graphite in the ductile cast irons with both matrix structures can be neglected. In the ductile cast iron with ferritic matrix, the grain size of ferritic matrix far from the spherical graphite is close to the wave length, which resulted in a large stochastic scattering. In the pearlitic matrix, however, the grain size of pearlite with lamellar structures far from the spherical graphite is much smaller than the ultrasonic wavelength, which brought a small stochastic scattering. On the contrary, because the anisotropy of the pearlite with lamellar structures is higher than that of the ferrite [16, 17], the Rayleigh scattering in the pearlitic matrix is larger than that of the ferritic matrix. Consequently, although the Rayleigh scattering in the ferritic matrix is smaller than that of the pearlitic matrix, the sum of the stochastic scattering and the Rayleigh scattering was larger than that of the pearlitic matrix, which accordingly predominated in the total ultrasonic attenuation of the ductile cast iron with ferritic matrix.

Conclusion

In this study, the effect of matrix structure on the ultrasonic attenuation of ductile cast irons was investigated by means of ultrasonic echo waves. The maximum ultrasonic attenuations, 0.077 dB/mm and 0.090 dB/mm, were obtained in the ductile cast irons with ferritic and pearlitic matrices, respectively. For similar frequencies, however, the ultrasonic attenuation in the ductile cast iron with pearlitic matrix was larger than that of the ferritic matrix. Combined with the theory of ultrasonic attenuation in the solid, the absorption loss and the scattering loss which included the stochastic scattering and Rayleigh scattering were calculated in the both ductile cast irons with ferritic and the pearlitic matrices. It indicated that in the ductile cast iron with ferritic matrix, the total ultrasonic

attenuation was mainly caused by the scattering losses. On the contrary, the absorption loss predominated in the total ultrasonic attenuation of the ductile cast iron with pearlitic matrix.

Acknowledgements This work was carried out under the financial supports of the Special Coordination Funds of Ministry, Culture, Sports, Science and Technology of Japanese Government.

References

1. Flemings MC (1974) Solidification processing. McGraw-Hill, USA, p 338
2. Kumar A, Laha K, Jayakumar T, Bhanu Sankara Rao K, Raj B (2001) Metall Mater Trans A 33A:1617
3. Kumar A, Laha K, Jayakumar T, Bhanu Sankara Rao K, Raj B (2002) Phi Mag A 82:2529
4. Rosen M, Ives L et al (1985) Mater Sci Eng 74:1
5. Lee SC, Suen JM (1989) Metall Trans A 20A:2399
6. Papadakis EP (1968) J Acoust Soc Am 44:1437
7. Seki H, Granato A, Truell R (1956) J coust Soc Am 28:230
8. Roderick RL, Truell R (1952) J Appl Phys 23:267
9. Papadakis EP (1966) J Acoust Soc Am 40:863
10. Krautkramer J, Krautkramer H, Grabendorfer W, Niklas L (1977) Ultrasonic testing of materials. Springer, Berlin, p 116
11. Mason WP, Mcskimin HJ (1947) J Acoust Soc Am 19:464
12. Mason WP, Mcskimin HJ (1948) J Appl Phys 19:940
13. Bhatia AB (1959) J Acoust Soc Am 31:16
14. Bhatia AB, Moore RA (1959) J Acoust Soc Am 31:1140
15. Adams RD, Fox MAO (1973) J Iron and Steel Int 37:4028
16. Papadakis EP (1964) J Acoust Soc Am 36:1474
17. Kamigaki K (1957) Sci Rep Tohoku Univ First Ser A 9:48